PCCP

Dynamic Article Links

Cite this: *Phys. Chem. Chem. Phys.*, 2012, **14**, 16552–16557

www.rsc.org/pccp

PAPER

The role of titanium nitride supports for single-atom platinum-based catalysts in fuel cell technology†

Ren-Qin Zhang,[a] Tae-Hun Lee,[a] Byung-Deok Yu,[b] Catherine Stampfl[c] and Aloysius Soon*[a]

Received 17th April 2012, Accepted 14th June 2012
DOI: 10.1039/c2cp41392b

As a first step towards a microscopic understanding of single-Pt atom-dispersed catalysts on non-conventional TiN supports, we present density-functional theory (DFT) calculations to investigate the adsorption properties of Pt atoms on the pristine TiN(100) surface, as well as the dominant influence of surface defects on the thermodynamic stability of platinized TiN. Optimized atomic geometries, energetics, and analysis of the electronic structure of the Pt/TiN system are reported for various surface coverages of Pt. We find that atomic Pt does not bind preferably to the clean TiN surface, but under typical PEM fuel cell operating conditions, *i.e.* strongly oxidizing conditions, TiN surface vacancies play a crucial role in anchoring the Pt atom for its catalytic function. Whilst considering the energetic stability of the Pt/TiN structures under varying N conditions, embedding Pt at the surface N-vacancy site is found to be the most favorable under N-lean conditions. Thus, the system of embedding Pt at the surface N-vacancy sites on TiN(100) surfaces could be promising catalysts for PEM fuel cells.

Introduction

Heterogeneous catalysis has received a tremendous amount of interest, both from a scientific and industrial perspective. Due to the enormous scale of commercial applications, progress in catalysis can have a positive economic as well as environmental impact, particularly in the area of clean energy technologies. More specifically, the automotive and power generation (*e.g.* fuel cells) industries are the sectors that stand to benefit most directly from breakthroughs that are expected to occur in the field of catalysis. Amongst the various types of fuel cells studied thus far, proton exchange membrane fuel cells (PEMFCs) have received broad attention due to their low operating temperature, low weight, low emissions and quick start-up time.[1,2] However, there still exist some challenges that hinder their large-scale commercialization, such as the use of the expensive platinum (Pt) catalyst, carbon monoxide (CO) poisoning of this Pt catalyst, as well as severe carbon electrode corrosion.[3] In essence, two major drawbacks for the efficient use of PEMFC are namely, its high production costs (due to the use of the Pt catalyst) and its low material durability (resulting in poor lifecycling).[4] In order to increase the efficiency on a per Pt atom basis in Pt-based heterogeneous catalysts, one may attempt to increase the surface-to-volume ratio of Pt-based nano-catalysts – confining Pt to the surface as surface-active atoms. There have been various approaches concerning the reduction of Pt *via* nanostructing, such as decreasing the size of Pt nanoparticles,[1,4] using a monolayer of Pt in core–shell nanoparticles,[5,6] or replacing it with non-Pt metals for electrode fabrication.[3,7]

Another aspect that greatly influences the performance of an electrocatalyst is the nature of the support material. Given the harsh corrosive operational conditions of the PEMFC, the search is on for high-performance, durable materials that are required to withstand the degradation caused due to acidic and oxidizing conditions. The ideal catalyst support material should thus be corrosion-resistant under strongly oxidizing conditions of the PEMFC. Known for its good electrical conductivity and its high resistance to corrosion and acid-attack,[8] titanium nitride (TiN, see Fig. 1a) is thus considered one of the best candidates for the metallic support material in PEMFCs,[9] and methanol direct fuel cells,[10] demonstrating clear advantages over traditionally used carbon-based supports which are prone to electrode degradation in a strong acidic medium.[1] In particular, nanoparticles of TiN have been used as a catalyst support material for PEMFCs and they demonstrate higher catalytic performance than conventional platinized carbon electrocatalysts.[11] Also, TiN has been proposed as a substrate for electrodeposition of metals such as Pt and Pd.[12–14] However, detailed surface mechanisms (at the atomic-scale) are still clearly lacking which are crucial for durable materials development.

[a] *Department of Materials Science & Engineering, Yonsei University, Seoul 120-749, Korea. E-mail: aloysius.soon@yonsei.ac.kr*
[b] *Department of Physics, University of Seoul, Seoul 130-743, Korea*
[c] *School of Physics, The University of Sydney, Sydney NSW 2006, Australia*

† This article was submitted as part of a collection on Computational Catalysis and Materials for Energy Production, Storage and Utilization.

This journal is © the Owner Societies 2012

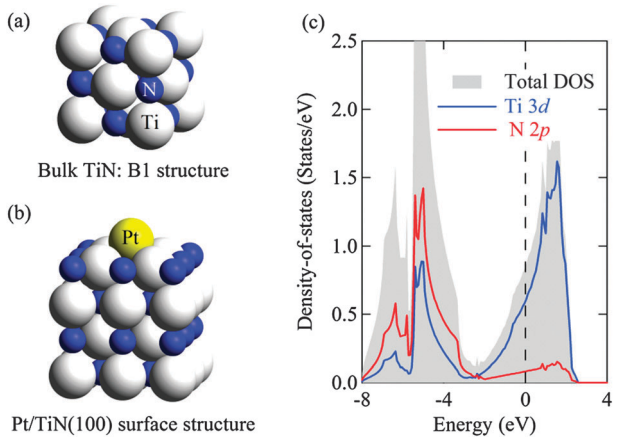

Fig. 1 The crystal structure of bulk titanium nitride, TiN, and the atomic structure model of Pt embedded in an N vacancy site on the TiN(100) surface are shown in (a) and (b), respectively. The platinum, titanium and nitrogen atoms are shown as large yellow, large white and small blue spheres, respectively. (c) The calculated partial density-of-states (PDOSs) of bulk TiN. The Fermi energy is indicated by the vertical dashed line at 0 eV.

In view of all the above-mentioned requirements, we hereby propose one possible design strategy, *i.e.* to combine the use of a durable support material such as TiN and to employ the concept of "single-atom" catalysis which will attempt to reduce the loading of the Pt catalyst in PEMFCs, as well as increasing its per-atom efficiency.

The concept of "single-atom catalysis" was first coined by Sir John Meurig Thomas.[15] The single-atom catalyst not only has an extremely high atom efficiency and activity,[16] but is also a promising way to reduce the high cost of commercial noble-metal catalysts in industry. Recently, Qiao *et al.* have demonstrated experimentally that single Pt atoms could be uniformly dispersed on an FeO_x support of high surface area.[17] The stabilization of single Pt atoms is believed to be due to the electron transfer from Pt atoms to the FeO_x surface. This charge-transfer mechanism could well be extended to other substrates,[19,20] *e.g.* a nitride support which is studied in this work.[18,19] Electrodeposition of Pt metal on TiN substrates[20] also shows good electrical conductivity of, and connectivity between, the deposited Pt and the TiN substrate. Thus, single Pt atoms dispersed on the TiN substrate is expected to be a promising electrode system for PEMFCs.[21] However, again, an atomic-level understanding of the Pt/TiN system is still unknown, such as the explicit chemistry for on-surface anchoring or in-surface embedding of Pt atoms on the TiN support.

It is evident that first-principles density-functional theory (DFT) calculations have a distinct advantage of investigating the energetics of atomic-level processes (*e.g.* in heterogeneous catalysis) with high-level precision, as well as providing quantum mechanical-based insights to the associated electronic structure of these processes, *e.g.* how electron transfer could affect the reactivities of Pt/substrate catalysts.[18,23] Thus, in this work, we use first-principles DFT calculations to understand the fundamental properties of the Pt/TiN electrode system to aid in the rational design of the next generation of PEMFCs. Optimized atomic geometries, energetics, and analysis of the electronic structure of the Pt/TiN system are reported for various surface coverages of Pt. We find that atomic Pt does not bind preferably to the clean TiN(100) surface, but under typical PEM fuel cells operational conditions, *i.e.* strongly oxidizing conditions,[3,4] TiN surface vacancies (*e.g.* V_N) play a crucial role in anchoring the Pt atom for its catalytic function.

Computational method

For all DFT calculations, we use the Vienna *Ab initio* Simulations Package (VASP 5.2) code.[22,23] We employ the projector augmented-wave (PAW) method[24] for the electron–ion interactions and the generalized-gradient approximation (GGA) due to Perdew, Burke and Ernzerhof (PBE)[25] for the exchange–correlation functional. With its PAW potentials, VASP combines the accuracy of all-electron methods with the computational efficiency of plane-wave approaches. The electronic wave functions are expanded in a basis set of plane waves with a kinetic-energy cutoff of 500 eV. In order to study the effect of the adsorption of Pt atoms on the electronic structure and properties of the TiN(100) surface as a function of surface coverage Θ, we use a periodic slab model consisting of four atomic layers with a vacuum region of about 12 Å (See Fig. 1b). We find that upon increasing the number of atomic layers to six layers, the difference in binding energy is found to be less than 0.02 eV/Pt atom. The different surface coverages are modeled using $p(1 \times 1)$, $p(2 \times 2)$, $p(3 \times 3)$, $p(4 \times 4)$ surface cells, where we consider $\Theta = 0.06$ to 1.00 ML. We define Θ as the ratio of the number of Pt atoms to the number of TiN units in the unit cell of an ideal TiN surface. Pt atoms and the top two atomic layers are allowed to fully relax while keeping the bottom two layers fixed. We consider adsorption in various on-surface sites and surface vacancy sites (substitutional adsorption). The **k**-space integration is performed using $12 \times 12 \times 1$, $6 \times 6 \times 1$, $4 \times 4 \times 1$, $3 \times 3 \times 1$ meshes in the Brillouin zone for the $p(1 \times 1)$, $p(2 \times 2)$, $p(3 \times 3)$, $p(4 \times 4)$ surface cells, respectively. A Methfessel-Paxton smearing of 0.1 eV is used to improve the convergence and the total energy is extrapolated back to zero temperature. Dipole corrections[26] to the electrostatic potential and total energy are imposed to eliminate dipole–dipole interactions of images between supercells. The convergence criterion for the total energy is taken to be smaller than 1×10^{-5} eV, while for geometry optimization, the ionic relaxations are performed until the net change in the forces acting on the atoms becomes smaller than 1×10^{-2} eV Å^{-1}.

In order to investigate the thermodynamic stability of Pt adsorption in on-surface sites and surface vacancy sites, we define the average binding energy per Pt atom, E_{Pt}^{b}. To address the possibility of bulk-like clustering behavior of Pt on TiN(100), E_{Pt}^{b} is calculated with respect to the total energy of bulk Pt E_{Pt}^{bulk}. The chemical potentials of N under different chemical environments can strongly affect the properties of Pt/TiN surfaces. Given that the operating conditions of PEMFCs are typically under strongly oxidizing conditions,[3,4] in this work we will address the stability of the Pt/TiN(100) structures under low chemical potential of N, μ_N conditions as a first approximation to these harsh oxidizing conditions. To estimate the thermodynamic stability of single Pt atoms adsorbed on clean and defective surfaces of TiN(100), the binding energy of Pt, E_{Pt}^{b}, is calculated,

including the cost of vacancy formation energy, as a function of the chemical potential of N, μ_N. It is defined as

$$E_{Pt}^{b} = E_{tot} - E_{TiN}^{clean} - (n\mu_{Ti} + m\mu_N + l\mu_{Pt}) \quad (1)$$

where E_{tot} and E_{TiN}^{clean} are the total energy of the system for Pt adsorbed on a vacancy site and pure TiN (surface or bulk), respectively; n, m and l are the number of the Ti vacancies, N vacancies and adsorbed Pt atoms, respectively. μ_{Ti}, μ_N and μ_{Pt} are the atomic chemical potentials of the Ti, N and Pt, respectively. Here we assume μ_{Pt} as the binding energy of bulk Pt E_{Pt}^{bulk}. The lower boundary (*i.e.* under N-lean conditions), is taken as the chemical potential of N whereby the spontaneous decomposition of the nitride into titanium metal and nitrogen gas will become favorable, whereas that of the upper boundary (*i.e.* under N-rich conditions) is defined when N_2 condensation takes place on the surface at low temperatures. Thus, under N-lean conditions, $\mu_{Ti} = E_{Ti}^{bulk}$ and $\mu_N = E_{TiN}^{bulk} - E_{Ti}^{bulk}$, while under N-rich conditions, $\mu_N = \frac{1}{2}E_{N_2}^{mlc}$ and $\mu_{Ti} = E_{TiN}^{bulk} - \frac{1}{2}E_{N_2}$, where E_{TiN}^{bulk}, E_{Ti}^{bulk} and $E_{N_2}^{mlc}$ are the total energies of bulk TiN, bulk Ti and the N_2 molecule, respectively. We note that for the stability of a single Pt adsorption in on-surface sites (*i.e.* without vacancy), the binding energy can be calculated by eqn (1) when $n = 0$ and $m = 0$, with $\mu_{Pt} = E_{Pt}^{bulk}$ consistently referred to that of bulk Pt. In eqn (1), a positive binding energy indicates that the adsorption is endothermic, while a negative binding energy indicates that the adsorption is exothermic and thermodynamically more stable than that in bulk Pt.

Results and discussion

Firstly, we calculate the properties of bulk TiN, yielding a lattice constant of 4.249 Å and bulk modulus of 280 GPa, which is consistent with the experimental results of 4.238 Å[27] and 288 GPa,[28] respectively, as well as the theoretical values of 4.210 Å and 275.5 GPa in our previous work.[29] The electronic density-of-states, decomposed into Ti 3d and N 2p states, are shown in Fig. 1c, which shows that TiN is a metal with 0.87 states eV^{-1} at the Fermi level.[8] The largely dispersive unoccupied bands are composed of Ti 3d states, while the occupied bands show a strong hybridization of N 2p–Ti 3d states.

The calculated binding energies with respect to the energy of bulk Pt (per Pt atom) vary as function of the surface coverage Θ, which is presented in Fig. 2. For on-surface adsorption at each of the surface coverages, Pt atoms are placed in the top sites (T_{Ti} and T_N) and bridge sites (B_{AA} and B_{AB}), as shown in the insert of Fig. 2. It is found that as Θ increases from 0.06 to 0.25 ML, the binding energy at all adsorption sites increases, while for increasing Θ to 1.0 ML, the binding energy decreases. This dramatic variation is attributed to the competition between the Pt-surface and lateral Pt–Pt interactions. When compared to the cohesive energy of bulk Pt, the positive binding energies of Pt at the considered on-surface sites suggest that the cohesive energy of Pt atoms on TiN(100) is less favorable than that in bulk Pt. This suggests that single Pt atom adsorption at these sites is thermodynamically unstable, and driving the atoms to form more favorable bulk-like Pt clusters. Here, we also find adsorbed Pt atoms on TiN(100) are displaced vertically away from the surface by 2.14, 2.28, 2.02, and 2.22 Å for the B_{AA}, B_{AB}, T_N, and T_{Ti} sites, respectively (*e.g.* at the 0.06 ML coverage).

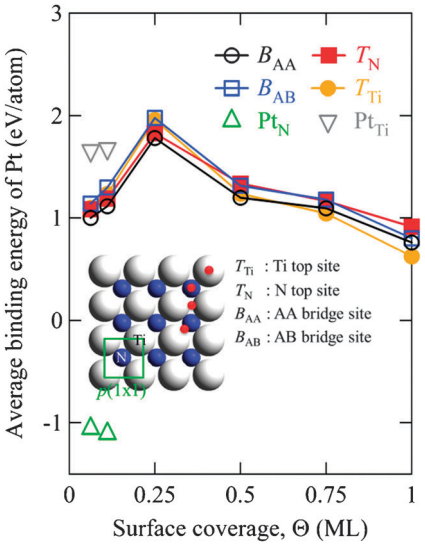

Fig. 2 Calculated binding energies of Pt on TiN(100) surface (calculated by eqn (1)) in the on-surface sites for various coverages. B_{AA}, B_{AB}, T_N and T_{Ti} denote the on-surface adsorption sites of AA bridge (*i.e.* a bridge site between two like atoms), AB bridge (*i.e.* a bridge site between an N atom and a Ti atom), N top and Ti top, respectively (as shown in the insert), while Pt_N and Pt_{Ti} denote the substitutional adsorption sites of N and Ti vacancies, correspondingly. For the substitutional adsorption, the binding energies calculated by eqn (1) under N-lean conditions for Pt_N and N-rich conditions for Pt_{Ti} are shown. For the cases under N-rich conditions for Pt_N and N-lean conditions for Pt_{Ti}, the binding energies are large and positive values (see Table 2).

However, we note that previous theoretical calculations have reported that nitrogen point defects could influence the stability and induce atomic-scale structural changes in transition-metal nitrides.[30] Furthermore, recent studies of iron oxide supported single Pt atoms show that surface vacancies of the supports could well serve as anchoring sites for single Pt atoms.[17] In this work, we study the N (V_N) and Ti (V_{Ti}) atom vacancy formation energies of TiN(100) surface and bulk TiN under different nitrogen environments (N-lean and N-rich), which are listed in Table 1. The vacancy formation energy is calculated by eqn (1) when $l = 0$. We find that N vacancies form readily and are exothermic both on the surface and in the bulk under N-lean conditions. Under such conditions, Ti vacancy formation at both the surface and in the bulk is found to be largely endothermic and has a considerable formation

Table 1 The N (V_N) and Ti (V_{Ti}) vacancy formation energy for vacancies at the TiN(100) surface and in bulk TiN, under different conditions (N-lean and N-rich). $p(3 \times 3)$ and $p(4 \times 4)$ are the size of the surface unit cell, which represents different vacancy surface coverages of 0.11 and 0.06 ML, respectively. For bulk TiN, a $(3 \times 3 \times 3)$ supercell is used, which is found to be sufficiently large to exclude the interaction between vacancies (we have checked with a bulk $(4 \times 4 \times 4)$ supercell and the conclusion was not changed)

V_N (eV)	N-lean	N-rich	V_{Ti} (eV)	N-lean	N-rich
$p(3 \times 3)$	−0.42	3.02	$p(3 \times 3)$	3.40	−0.04
$p(4 \times 4)$	−0.37	3.07	$p(4 \times 4)$	3.45	0.00
Bulk $(3 \times 3 \times 3)$	−0.87	2.58	Bulk $(3 \times 3 \times 3)$	2.96	−0.49

This journal is © the Owner Societies 2012

energy of ~3–3.5 eV. On the other hand, under N-rich conditions, N vacancies are difficult to form, yielding a large formation energy of ~2.5–3 eV. The formation of Ti vacancies, however, is found to be slightly easier than that of N vacancies, but their formation energy is marginally exothermic. We have also found that a nitrogen mono-vacancy is considerably easier to form on TiN(100) than a di-vacancy, under N-lean conditions.[31]

The high stability of surface vacancies under certain conditions has prompted us to further investigate the adsorption properties of Pt at these sites. We considered so-called substitutional adsorption of Pt atoms in the Ti and N vacancy sites, which are labeled Pt_{Ti} and Pt_N, respectively. Again, as shown in Fig. 2, the binding energies at all other considered sites are always positive with respect to that of bulk Pt, with the exception of Pt adsorption at the N vacancy site (Pt_N) under N-lean conditions. This leads us to believe that the binding of Pt to TiN surfaces is strongly mediated *via* these surface V_N, highlighting the importance of surface defects for this system. When compared to the cohesive energy of bulk Pt, the negative binding energy of Pt at V_N implies that the cohesive energy of a Pt atom on defective TiN(100) is higher than that of bulk Pt atoms. Nevertheless, the positive binding energy of Pt adsorption at V_{Ti} under N-rich conditions denotes that the Ti vacancy site is unfavorable for Pt adsorption, even when compared to on-surface Pt adsorption. Concerning the atomic structures, for the Pt_N system, the vertical displacement of Pt from the TiN(100) surface is found to be 1.41 Å (and bond length of Pt–Ti, d_{Pt-Ti} is 2.66 Å), while that of the Pt_{Ti} system is found to be 0.30 Å (and d_{Pt-N} is 2.17 Å).

In a nutshell, Pt atoms prefer to be "embedded" on the surface of TiN(100) only at the V_N site, while all other on-surface adsorptions are largely unfavourable with respect to bulk Pt. This somewhat resembles the result of Pt single atoms bound to the Fe_2O_3 surface, as seen in experiments.[17]

Given that the diffusion of Pt into the carbon supports is one of the well-known reasons for poor efficiencies of Pt/carbon catalysts, we find it necessary to check the thermodynamic stability of Pt atoms in bulk TiN. To check this, we calculate the binding energy of Pt_{Ti} and Pt_N in bulk TiN using a (3 × 3 × 3) bulk TiN supercell, *i.e.* substituting a Pt atom at the Ti, and N site, respectively. In Table 2, we list the atomic binding energy of Pt atoms adsorbed on the N and Ti surface vacancy sites under N-lean and N-rich conditions, compared to that in bulk TiN. For Pt in both the N and Ti vacancy sites of bulk TiN, the positive and large binding energies indicate that it is thermodynamically very unlikely for Pt atoms to occupy N and Ti sites of bulk TiN. These large positive values are attributed to the large size mismatch between Pt and the smaller N and Ti atoms in bulk TiN. In addition, the binding energies of Pt_N at the TiN surface are very similar for both the $p(3 \times 3)$ and $p(4 \times 4)$ surface unit cells, *i.e.* for coverages of 0.11 and 0.06 ML, respectively. This indicates that the $p(3 \times 3)$ surface unit cell should be large enough to minimize the lateral interactions between Pt atoms. Thus, we can conclude that Pt atoms can be stably embedded in the N vacancy site of TiN(100) surface, without forming bulk-like Pt clusters, nor diffusing into bulk TiN. From a thermodynamic point-of-view, the Pt/TiN system could offer a possible route to improve the efficiencies of Pt-based nanocatalysts for the PEMFC.

Table 2 The binding energy of Pt atoms adsorbed on N and Ti vacancy sites at the TiN(100) surface and in bulk TiN, which are denoted by Pt_N and Pt_{Ti} , respectively (calculated by eqn (1)). $p(3 \times 3)$ and $p(4 \times 4)$ are the surface unit cells used, which represent different Pt surface coverages of 0.11 and 0.06 ML, respectively. For bulk TiN, a supercell of (3 × 3 × 3) is used, containing 54 atoms, which is large enough to exclude the interaction between Pt atoms

	Pt_N		Pt_{Ti}	
E_{Pt}^b (eV)	N-lean	N-rich	N-lean	N-rich
$p(3 \times 3)$	−1.11	2.33	5.12	1.68
$p(4 \times 4)$	−1.06	2.38	5.11	1.66
Bulk (3 × 3 × 3)	3.44	6.89	7.64	4.19

In Fig. 3, with increasing chemical potential of N, μ_N, *i.e.* from N-lean to N-rich conditions, the binding energy of Pt at the N vacancy increases, while that of Pt at the Ti vacancy decreases. It can be seen that when $\Delta\mu_N < -2.33$ eV, Pt_N at TiN(100) is the only system for which the binding energy is found to be negative, *i.e.* thermodynamically stable. With increasing μ_N, the binding energy of Pt_N at TiN(100) increases and finally becomes positive and larger than that of Pt adsorbed on the surface of clean TiN(100) (average on-surface adsorption: $E_b = 1.21$ eV) when $\Delta\mu_N > -1.12$ eV. Thus, it can be inferred that Pt at the surface N-vacancy is the most favorable system under N-lean conditions, and as μ_N increases, it becomes increasingly less favorable, and ends up being less stable than the on-surface adsorption systems. Considering the energetic stability of the Pt/TiN structures under varying N conditions, it is concluded that embedding Pt at the surface N-vacancy site is the most favorable under N-lean conditions,

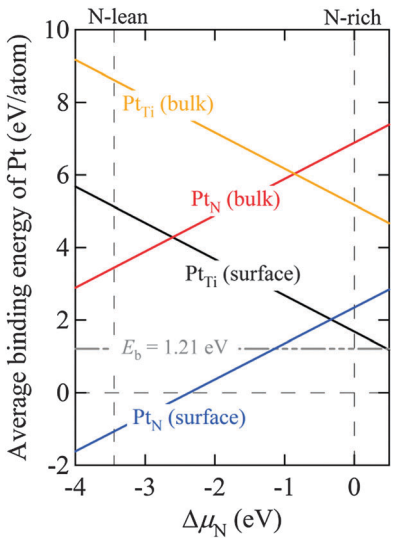

Fig. 3 According to eqn (1), the binding energy of Pt, E_{Pt}^b, in the bulk and surface N- and Ti-vacancy sites changes as a function of chemical potential of N, μ_N, for the (3 × 3 × 3) bulk TiN and the $p(3 \times 3)$ TiN(100) systems. $\Delta\mu_N$ is defined by $\Delta\mu_N = \mu_N - \frac{1}{2}E_{N_2}^{mlc}$, where $E_{N_2}^{mlc}$ is the total energy of the N_2 molecule. The thermodynamically allowed range of $\Delta\mu_N$ is between −3.45 eV (N-lean) and 0.00 eV (N-rich). Pt_N and Pt_{Ti} denote the substitutional adsorption sites of N and Ti vacancies in the TiN bulk and surface, respectively. The dot dashed line denotes the average binding energy of Pt for the situation of on-surface adsorption of the $p(3 \times 3)$ TiN(100) system, in the most favorable site, which is 1.21 eV.

which seems to be a reasonable first approximation to strongly oxidizing conditions (*i.e.* close to PEMFC operating conditions).

To provide further insight into the electronic structure of the systems, we consider the partial density-of-states of Pt atoms adsorbed in both Ti and N vacancy sites, as shown in Fig. 4. In both cases, we observe a renormalization of Pt 5d states, compared with Pt 5d states of the clean Pt(100) surface and bulk Pt. The stability of Pt adsorbed on the N vacancy site is reflected in the lower energy position of the electronic states, which are mainly distributed in the range from −3 to −2 eV, compared to that of Pt adsorbed on the Ti vacancy site, which are mainly distributed in the range from −2 to −1 eV. We also calculated the d band centre, ε_d, of Pt and Ti atoms in the different systems, as shown in Table 3. For Pt_N, the ε_d of Pt 5d bands in the Pt_N system is lower than that of the Pt_{Ti} system, because of the interaction between Pt 5d states and Ti 3d states. Simultaneously, the ε_d of the Ti 3d bands for the Pt_N adsorption is higher than that of the Ti 3d bands of the clean TiN(100) surface and bulk TiN.

To further aid our understanding, we discuss this difference *via* plots of charge density differences, as shown in Fig. 5 for the Pt atoms adsorbed on N and Ti vacancy sites of the TiN(100) surface systems. The charge density difference, $\Delta\rho$, can be derived by considering: $\Delta\rho = \rho^{sys} - \rho^{Pt} - \rho^{TiN}$, where ρ^{sys}, ρ^{Pt} and ρ^{TiN} are the charge densities of the supercell Pt/TiN slab system, the Pt atom and the slab of TiN(100) surface with N (or Ti) vacancy, respectively. In calculation of the latter two quantities, the atomic positions are fixed as those they have in the Pt/TiN system. From these redistributions, it is found that for Pt_N, there is a bonding between the Pt and Ti atoms. As we can see, the depletion (blue) of electron density on both the Pt and Ti atoms, and a significant (yellow) accumulation between them. There is a "ring" of negative charge about the Pt atom, which is consistent with our calculated Bader charge result (−0.49|*e*|). For Pt atoms adsorbed on an N vacancy site, it suggests that a single Pt atom embedded into the TiN surface experiences a significant increase in the occupation of the 5d states due to coordination by the four neighboring surface Ti atoms, where the electronegativity of Pt (Pauling value of 2.28) is larger than that of Ti (Pauling value of 1.54). The charge transfer is localized around Pt and Ti atoms. For Pt atom adsorption on Ti vacancies, the charge redistribution is directional and both N and Ti atoms are involved in the charge transfer. Also, there is some kind of directional interaction between the Pt and N atoms; one of the main effects is considered to be a depletion of the planar Pt 5d states, and increase into the perpendicular d_{zz} states. This could give rise to the (presumably) anti-bonding type Pt states at/near the Fermi level (seen in Fig. 4b), which result in the unfavorable Pt adsorption energy.

As a first step towards the atomic and electronic understanding of single-Pt atom-dispersion on TiN surfaces for catalysts in

Table 3 The d-band centre, ε_d, with respect to the corresponding Fermi level for the different systems. Pt_{Ti} and Pt_N denote the systems of Pt adsorbed on Ti and N vacancy sites in the TiN(100) surface, respectively

ε_d (eV)	Bulk Pt	Clean Pt(100)	Pt_{Ti}	Pt_N	Clean TiN(100)	Bulk TiN
Pt	−3.092	−2.118	−2.158	−2.746	—	—
Ti	—	—	—	−3.946	−4.074	−4.606

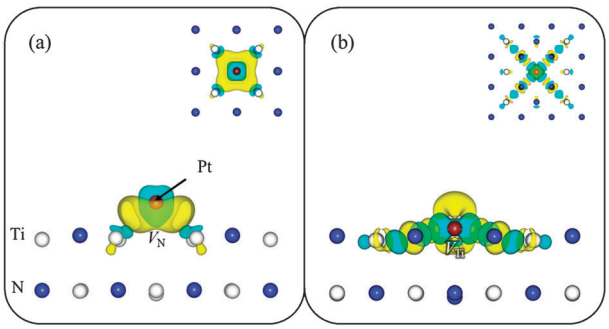

Fig. 5 A side-view of electron charge density differences for the substitutional adsorption of Pt atoms on the (a) N and (b) Ti vacancy sites, respectively, where the inset shows the corresponding top-view. Charge accumulation and depletion are represented by the yellow and light blue regions, respectively. The isosurface levels are set to ±0.005 e $bohr^{-3}$.

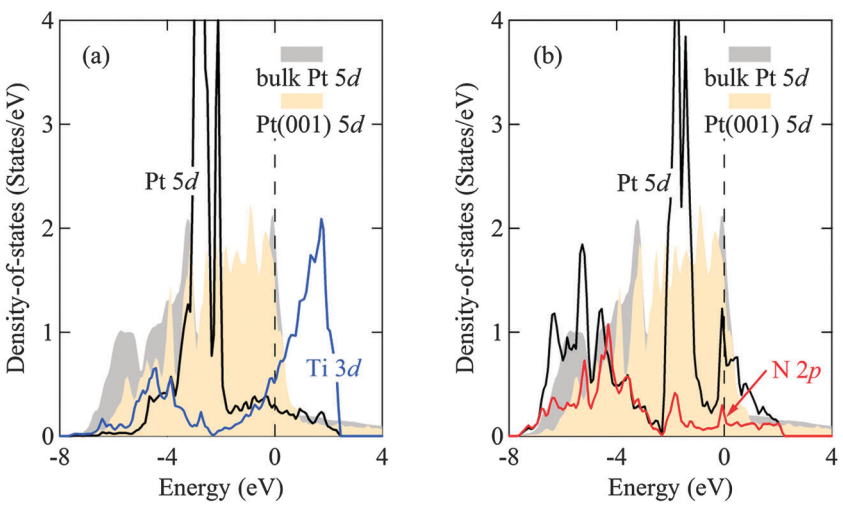

Fig. 4 The partial density-of-states for Pt atoms adsorbed on (a) an N vacancy site, and (b) a Ti vacancy site. The Fermi energy is indicated by the vertical dash line at 0 eV.

This journal is © the Owner Societies 2012

PEMFC, by using first-principle calculations, we study the stability of single-Pt atoms on the (100) surface of the non-conventional support material TiN. Single-Pt atoms prefer to occupy the N vacancy sites in the TiN surface under N-lean conditions. In order to realize the application of this platinized TiN surface in PEMFCs, further research is being pursued to investigate the stability of Pt/TiN electrodes in different electrolytes *via* surface Pourbaix diagrams.

Conclusion

In summary, utilizing first-principles DFT calculations, TiN supports for single-atom platinum-based catalysts are investigated. It is found that a Pt atom prefers to be embedded in the surface of TiN at the N vacancy sites. According to the binding energy of Pt atoms, with respect to that of bulk Pt, single Pt atoms could be stable on the N atomic vacancy site rather than forming Pt metal clusters. The substitutional adsorption of Pt atoms at Ti vacancy sites in bulk TiN is energetically unfavorable. We found that atomic Pt does not bind preferably to the clean TiN surface, but under typical PEM fuel cells operational conditions, *i.e.* strongly oxidizing conditions, TiN surface vacancies play a crucial role in anchoring the Pt atom for its catalytic function. Whilst considering the energetic stability of the Pt/TiN structures under varying N conditions, embedding Pt at the surface N-vacancy site is found to be the most favorable under N-lean conditions, where Pt presents negative charge.

Acknowledgements

The authors gratefully acknowledge support through a financial award provided by the Asian Office of Aerospace Research and Development (AOARD, Award No. FA2386-12-1-4017), and the Australian Research Council (ARC). Computational resources have been provided by the Korea Institute of Science and Technology Information (KISTI) supercomputing center through the strategic support program for the supercomputing application research (KSC-2011-C2-39), as well as the Australian National Computational Infrastructure (NCI). RQZ acknowledges the Second Stage of Brain Korea 21 Project (Division of Humantronics Information Materials) for funding.

References

1 D. Ham and J. Lee, *Energies*, 2009, **2**, 873–899.
2 D. Anne-Claire, *Prog. Mater. Sci.*, 2011, **56**, 289–327.
3 R. Bashyam and P. Zelenay, *Nature*, 2006, **443**, 63–66.
4 H. A. Gasteiger, S. S. Kocha, B. Sompalli and F. T. Wagner, *Appl. Catal., B*, 2005, **56**, 9–35.
5 M. H. Huang, G. F. Dong, N. Wang, J. X. Xu and L. H. Guan, *Energy Environ. Sci.*, 2011, **4**, 4513–4516.
6 K. A. Kuttiyiel, K. Sasaki, Y. Choi, D. Su, P. Liu and R. R. Adzic, *Energy Environ. Sci.*, 2012, **5**, 5297–5304.
7 Y. Liang, Y. Li, H. Wang, J. Zhou, J. Wang, T. Regier and H. Dai, *Nat. Mater.*, 2011, **10**, 780–786.
8 C. Stampfl, W. Mannstadt, R. Asahi and A. J. Freeman, *Phys. Rev. B: Condens. Matter*, 2001, **63**, 155106.
9 B. Avasarala and P. Haldar, *Electrochim. Acta*, 2010, **55**, 9024–9034.
10 M. M. Ottakam Thotiyl, T. Ravikumar and S. Sampath, *J. Mater. Chem.*, 2010, **20**, 10643–10651.
11 B. Avasarala, T. Murray, W. Li and P. Haldar, *J. Mater. Chem.*, 2009, **19**, 1803–1805.
12 O. T. M. Musthafa and S. Sampath, *Chem. Commun.*, 2008, 67–69.
13 M. M. O. Thotiyl, T. R. Kumar and S. Sampath, *J. Phys. Chem. C*, 2010, **114**, 17934–17941.
14 M. M. O. Thotiyl and S. Sampath, *Electrochim. Acta*, 2011, **56**, 3549–3554.
15 J. M. Thomas, R. Raja and D. W. Lewis, *Angew. Chem., Int. Ed.*, 2005, **44**, 6456–6482.
16 Y. Zhai, D. Pierre, R. Si, W. Deng, P. Ferrin, A. U. Nilekar, G. Peng, J. A. Herron, D. C. Bell, H. Saltsburg, M. Mavrikakis and M. Flytzani-Stephanopoulos, *Science*, 2010, **329**, 1633–1636.
17 B. Qiao, A. Wang, X. Yang, L. F. Allard, Z. Jiang, Y. Cui, J. Liu, J. Li and T. Zhang, *Nat. Chem.*, 2011, **3**, 634–641.
18 J. M. Thomas, Z. Saghi and P. L. Gai, *Top. Catal.*, 2011, **54**, 588–594.
19 J. H. Kwak, J. Hu, D. Mei, C.-W. Yi, D. H. Kim, C. H. F. Peden, L. F. Allard and J. Szanyi, *Science*, 2009, **325**, 1670–1673.
20 S. A. G. Evans, J. G. Terry, N. O. V. Plank, A. J. Walton, L. M. Keane, C. J. Campbell, P. Ghazal, J. S. Beattie, T.-J. Su, J. Crain and A. R. Mount, *Electrochem. Commun.*, 2005, **7**, 125–129.
21 J. M. Thomas, *Angew. Chem., Int. Ed.*, 2011, **50**, 49–50.
22 G. Kresse and J. Hafner, *Phys. Rev. B: Condens. Matter*, 1993, **47**, 558.
23 G. Kresse and J. Furthmüller, *Phys. Rev. B: Condens. Matter*, 1996, **54**, 11169.
24 G. Kresse and D. Joubert, *Phys. Rev. B: Condens. Matter Mater. Phys.*, 1999, **59**, 1758–1775.
25 J. P. Perdew, K. Burke and M. Ernzerhof, *Phys. Rev. Lett.*, 1996, **77**, 3865.
26 G. Makov and M. C. Payne, *Phys. Rev. B: Condens. Matter*, 1995, **51**, 4014.
27 N. Schönberg, *Acta Chem. Scand.*, 1954, **08**, 213–220.
28 M. Marlo and V. Milman, *Phys. Rev. B: Condens. Matter*, 2000, **62**, 2899.
29 R. Q. Zhang, C.-E. Kim, B. Delley, C. Stampfl and A. Soon, *Phys. Chem. Chem. Phys.*, 2012, **14**, 2462–2467.
30 L. Tsetseris, N. Kalfagiannis, S. Logothetidis and S. T. Pantelides, *Phys. Rev. Lett.*, 2007, **99**, 125503.
31 T.-H. Lee, B. Delley, C. Stampfl and A. Soon, *Nanoscale*, DOI: 10.1039/C2NR31266B.